



Research Article

Size-dependent catalytic property of gold nanoparticle mediated by *Justicia adhatoda* leaf extract

D. Latha¹ · P. Prabu³ · G. Gnanamoorthy¹ · S. Munusamy¹ · S. Sampurnam¹ · C. Arulvasu² · V. Narayanan¹

© Springer Nature Switzerland AG 2018

Abstract

In this contribution, we demonstrate the synthesis of gold nanoparticles (AuNPs) using an entirely green chemistry process. *Justicia adhatoda* leaf extract used as a bioreductant for the synthesis of AuNPs and its particle sizes are controlled by altering the concentration of metal salt. The optical and morphological properties were studied. We report on the synthesis of stable spherical, well-dispersed colloidal AuNPs (27.1, 33.3 and 46.8 nm) by efficient reducing agents with its mechanisms. The X-ray diffraction analysis also confirmed the obtained sizes of AuNPs with its crystallite size (20.2, 40.1 and 40.3 nm). Catalytic activity of fabricated AuNPs are also examined on the degradation of organic dyes.

Keywords *J. adhatoda* · AuNPs · Catalytic degradation · Methylene blue and Congo red

1 Introduction

Metallic nanoparticles have occupied an important place in the field of nanoscience due to their intriguing chemical, optical, electronic properties and etc. Metallic nanoparticles are synthesized by using reducing, protective and stabilizing agents. Such kind of agents are highly toxic, flammable, may adsorb on the surface of nanoparticles and are also unfavorable in their applications [1, 2]. Due to these confines, the researchers more concentrate on green approach for synthesis of nanoparticles. Several biological systems are existing for synthesis of metallic nanoparticles like as microbes, fungi, and plant materials. Recently, nanoparticles (silver, gold, copper, platinum, palladium etc.,) have been synthesized by using plants. This is due to large scale process, rapid synthesis and also produce more stable nanoparticles compare with other microorganisms. The development of green chemistry has three important factors, they are suitable solvent, ecofriendly reducing agent and non-toxic chemicals are used in synthesis of nanoparticles [3, 4]. Among various

metallic nanoparticles, researchers have more interest on gold nanoparticles (AuNPs) which is due to its unique properties, tunable SPR and applications [5].

Colloidal gold is a sol that exerted curative properties for several diseases [6]. Approximately 5.02 billion tons of gold produced by Philippines and ranked third in the world [7]. Gold nanoparticles have more commercial applications in various biomedical fields. Synthesized AuNPs have lot of applications like catalysis, cancer therapeutics, optical molecular sensing, electronics, optoelectronics, photonics diagnostic, drug delivery, biomedical sensing and imaging [8, 9]. Upon interacting with light, excited free electrons of AuNPs directly state to collective oscillation called as a strange Surface Plasmon Resonance (SPR) phenomenon [10, 11]. It can be tuned to different size or shape of the AuNPs, which cause the extensive investigation [12]. Various plant materials are used for synthesis of AuNPs such as *Magnolia kobus* & *Diopyros kaki* [13], *Acacia nilotica* [14], *Dillenia indica* [15], Edible mushroom [16] and *Cinnamomum zeylanicum* [17].

✉ V. Narayanan, vnnara@yahoo.co.in | ¹Department of Inorganic Chemistry, University of Madras, Guindy Campus, Chennai 600 025, India. ²Department of Zoology, University of Madras, Guindy Campus, Chennai, Tamilnadu 600 025, India. ³Department of Zoology, Pachaiyappa's College for Men, Kanchipuram, Tamilnadu 631 501, India.

In this study, we have examined the synthesis of AuNPs using medicinal plant *Justicia adhatoda* leaf extract, belongs to Acantheceae family. Phytochemical components of the leaf contain phenols, tannins, alkaloids, anthraquinones, saponins, flavonoids and reducing sugars, vasicine, vasicinone alkaloid and quinazoline [18–20]. The leaves of *J. adhatoda* contains considerable amount of alkaloids, flavonoids, phenols, proteins and carbohydrates (reducing sugar). These bioactive secondary metabolites are associated with their medicinal applications.

Pollution caused by heavy metals and dyes from industrial effluents are the chief origin of environmental pollution. In recent, more than 10,000 of different commercial dyes and pigments exist and about 7×10^5 tones are produced annually in worldwide [21–23]. It is expected that 10–15% of dye is lost during the dyeing process from the effluent. Dyes are broadly used in various industries like textile, color photography, pharmaceutical, food, cosmetics, paper, plastics and other industries [24]. They are using dye for coloring their products and discharge the effluents into water bodies. Such contaminated water is harmful to living organisms, in particularly Methylene blue and Congo red dye, it causes serious problem to the ecosystem [25, 26]. Methylene blue is a cationic dye and it is a heterocyclic aromatic compound ($C_{16}H_{18}N_3S$). Methylene blue can cause permanent injury to eyes, nausea, vomiting, diarrhea, skin irritation and severe serotonin toxicity [27, 28]. Congo red is a heterocyclic aromatic compound ($C_{32}H_{22}N_6Na_2O_6S_2$). It is a brownish-red crystal dye. It is chemically called as sodium salt of benzidine diazo-bis-1-naphthylamine-4-sulfonic acid. Congo red is a water soluble, highly stable and resistant to degrade. Congo red is a carcinogenic and cause irritation in skin, eye, gastrointestinal and also cause blood clotting, allergic reactions and respiratory problems [29, 30]. Numerous technologies and methods have been progressed for the removal of dyes from the industrial effluent. Various conventional methods existing such as coagulation, flocculation [31], ozonation [32], electrochemical method [33], fungal decolonization [34] adsorption on activated carbon [35–38], ultrafiltration and reverse osmosis are already in practice. These methods are costly, unsuccessful one and it cannot be effectively treated in broad range. Therefore, removal of these dyes are an important one, without using any other toxic chemicals. In recent decades, nano catalysts are attractive one to remove dyes from the industrial effluent. The nano catalyst is biocompatible, ecofriendly and facile route which is used to remove the dyes. Based on the above, the present study was focused on green synthesized AuNPs to evaluate their responsibility to degrade the dyes. We report on synthesise of stable AuNPs using leaf extract of *J. adhatoda* and project their size dependent

catalytic activity in dye degradation (Congo red and Methylene blue) process.

2 Methodology

2.1 Chemicals

$H AuCl_4 \cdot 3H_2O$ (99.9%), Congo red, Methylene blue, and Sodium borohydride were obtained from Sigma-Aldrich.

2.2 Preparation of aqueous leaf extract

The leaf of *Justicia adhatoda* was collected from Cumbum valley, Tamil Nadu, India and it is identified by experts. The leaves were washed with DD water three times to remove the dust particles and dried (shade, dry) for 10–14 days and ground into coarse powder. The coarse powder was refluxed at 80 °C for 20 min in a 250 mL Erlenmeyer flask containing 100 mL of DD water. After cooling, the extract was filtered through Whatman no. 1 filter paper and was kept in refrigerator for further use.

2.3 Synthesis of AuNPs

For synthesis of AuNPs, 1 mL aqueous extract was added to 7 mL of $H AuCl_4 \cdot 3H_2O$ (1 mM) with constant stirring for 10 min. The color of the reaction mixture changes from pale yellow to ruby red indicates the formation of gold nanoparticles due to the reduction of Au^{3+} to Au^0 , no precipitate was found. The synthesized gold nanoparticles were confirmed for the further characterizations.

2.3.1 Effect of metal ion concentration

One mL leaf extract was added to 7 mL of three different concentrations (0.5, 1.0 and 1.5 mM) of $H AuCl_4$, and synthesized AuNPs are labeled as a_1 , a_2 and a_3 respectively. The reduction and formation of AuNPs were monitored by using UV–Vis spectrophotometer.

2.3.2 Effect of different quantities of leaf extract on formation of AuNPs

Gold nanoparticles (AuNPs) were prepared by adding 1, 2 and 3 mL leaf extract of *J. adhatoda* with 7 mL of $H AuCl_4 \cdot 3H_2O$ (1 mM) independently, immediate pink-ruby red color was observed. The formation of AuNPs was monitored by UV–Vis spectrophotometer.

2.4 Characterization of AuNPs

The formation of the gold nanoparticles was recorded in the range of 700–400 nm is using UV–Visible spectrophotometer (Perkin Elmer Lambda-45). The size and shape of the nanoparticles were analyzed from SEM and TEM (Hitachi and TEM-JEOL model 1200EX) analyzer along with EDX operating at 200 kV. XRD analysis of the AuNPs was performed on Powder X-Ray Diffractometer (EnrafNonius CAD-4), operating at a voltage of 40 kV with Cu K α ($\lambda = 1.54 \text{ \AA}$) radiation.

2.5 Catalytic studies

2.5.1 Catalytic activity of Congo red degradation using AuNPs

The catalytic activity of AuNPs was evaluated against Congo red dye as a substrate in the presence of NaBH $_4$. For catalytic degradation, 1 mL of Congo red (1 mM) diluted with 10 mL of DD water and then 1 mL of freshly prepared NaBH $_4$ (0.1 and 0.2 M) was added respectively [39]. Size-dependent work was done by the addition of 500 μL colloidal AuNPs (a_1 , a_2 and a_3) with the mixture in UV light. The color of the samples gradually changed from deep red to colorless.

The catalytic activity of synthesized AuNPs was assessed against Methylene blue dye as a substrate in the presence of NaBH $_4$. In a typical assay, 1 mL of Methylene blue (1 mM) diluted with 10 mL DD water and then added to 1 mL of freshly prepared NaBH $_4$ [39, 40]. Two blank samples were prepared by various concentrations of NaBH $_4$ (0.1 and

0.2 M). The above procedures were repeated for the addition of a_1 , a_2 and a_3 of samples (500 μL) with Methylene blue in the presence of NaBH $_4$ separately. Finally, color changed into leuco Methylene blue color.

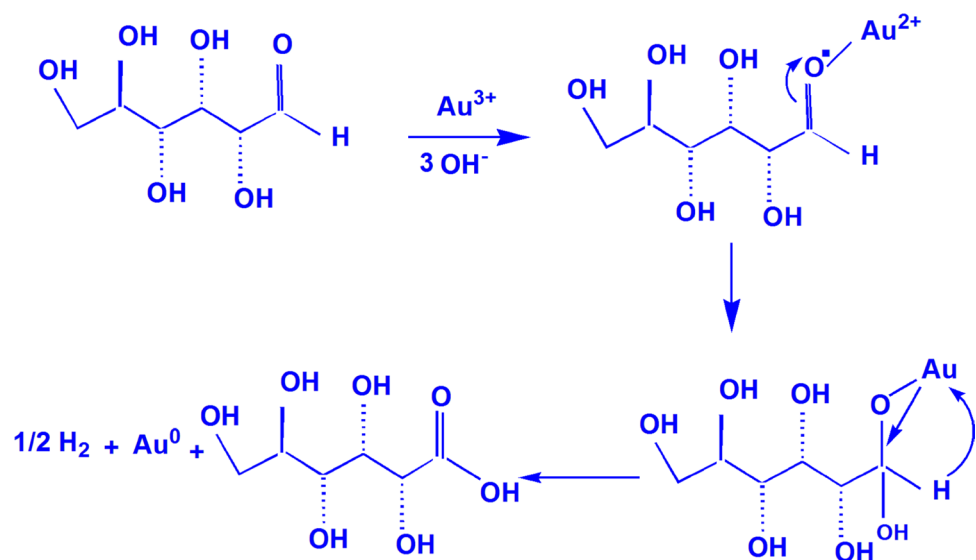
3 Results and discussion

Justicia adhatoda act as a biological reductor, to reduce gold chloride ions. The leaf of *J. adhatoda* constitutes water (15.3%), proteins (6.5%) and reducing sugar (16.4%) (D-glucose, D-galactose, β -glucoside-galactose, β -sitosterol-D-glucoside) [19]. During aqueous extract preparation, the reducing sugar broke down into smaller monosaccharide (glucose) unit exposing extra –CHO group [41]. The reducing activity of aldehyde group (–CHO) has been exploited by Tollens test, in which silver ions are reduced [42]. Similarly, the aldehyde group has reduced the gold ions into AuNPs. Maximum number of aldehyde group behave as a reducing agent for gold chloride ions [43].

3.1 *Justicia adhatoda* extract as a reducing agent for Au NPs

The possible redox reaction between gold ions and D-glucose has shown in schematic diagram (Fig. 1). It is continuously undergo nucleophilic substitution reaction, where O–H radicals present in the sixth carbon of glucose unit. First of all, Au $^{3+}$ ions gets attached with the oxygen of the aldehyde group present in glucose of aqueous extract, this is because of its free electrons. Due to instability of the carbon atom in the presence of O–H, those electrons gets

Fig. 1 Schematic diagram represents the reduction of Au $^{3+}$ ion into Au 0



transferred to Au^{3+} and gets reduced into Au^0 . At last, the oxygen of C=O group recovers the double bond and it is converted into gluconic acid [43].

3.2 *Justicia adhatoda* extract as a stabilizing agent for AuNPs

Silver (Ag) and gold (Au) nanoparticles are stabilized by hydroxyl (-OH) groups present in the starch molecules [44]. The terminal D-glucose unit gets oxidized into gluconic acid in the presence of Au ions. The negative charge of the gluconic acid interacts with the surface positive charge of AuNPs by electrostatic interaction; this is the reason for bond formation between them. Thus, the capping agent is responsible for AuNPs stabilization.

3.3 UV-Visible spectroscopy studies

3.3.1 Effect of contact time

Formation of gold nanoparticle (AuNPs) was monitored with the help of UV-Vis spectroscopy. A gradual color change could be observed from pale yellow to ruby red color after the addition of gold chloride solution which indicates the formation of AuNPs. The Surface Plasmon resonance (SPR) band is due to the oscillation of free conduction electrons induced by an interacting electromagnetic field on the surface of gold nanoparticles. The SPR band of AuNPs were related to their size, shape and aggregation conditions [45, 46]. The formation of AuNPs was confirmed by UV-Vis spectra (Fig. 2). The SPR peak is observed 542 nm which is gradually increased with the

function of time (10–60 min) and this is clearly exhibiting that the redox reaction has occurred between the aqueous extract and metal ions. Both of them were responsible for the formation of the stable AuNPs [47]. Early reports show that the temperature and pH parameters are vital factors which affecting the size and shape of the AuNPs [48–51]. The rate of formation of AuNPs increases with increase in the SPR band.

3.3.2 Effect of quantity of leaf extract

With an increasing ratio of leaf extract, subsequent color changes were noted from pink into reddish pink. In general, AuNPs is synthesized by direct deal with the quantity of aqueous extract, higher dosage of reducing agent will produce maximum yield of nanoparticle. The SPR peak of blue shift (542, 541 and 540 nm) for 1, 2 and 3 leaf extract respectively (Fig. 3). The formation of a blue shift indicates decreasing of the particle size [52–55].

3.3.3 Effect of metal concentrations

To examine the effect of metal salt concentration, the volume of leaf extract and HAuCl_4 were kept constant (1:7), but the concentration of metal salt varied (0.5, 1.0 and 1.5 mM). The rapid formation of dark pink color was noticed at high concentration of metal salt [56]. Figure 4 shows that the SPR peak intensity increases with increase in metal salt concentrations. The intensity of SPR peak and sharpness is increased at higher metal concentration which indicates increase of the size of nanoparticle [56, 58]. By increasing the metal concentration, increases

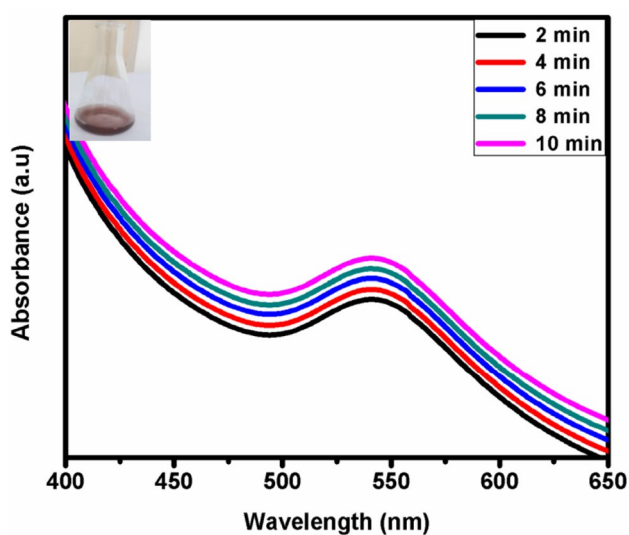


Fig. 2 UV-Vis spectra of AuNPs (Contact time for *J. adhatoda* leaf extract with HAuCl_4)

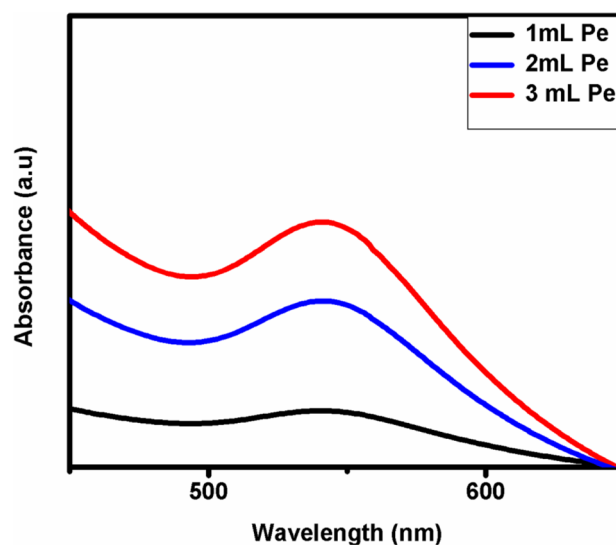


Fig. 3 UV-Vis spectra of AuNPs at different volume of *J. adhatoda* plant extract (PE)

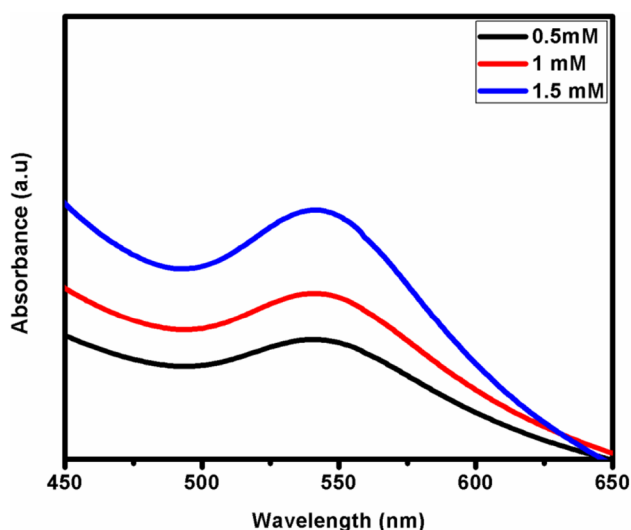


Fig. 4 UV-Vis spectra of AuNPs at various concentration of HAuCl_4 (0.5, 1.0 and 1.5 mM)

the size of AuNPs (a_1 – a_3) was also found in SEM and TEM images (Figs. 4 and 5). Dubey et al. [57] have also reported that the rate of formation of AuNPs was found to be faster at highest metal salt concentration. Dwivedi et al. [59] reported that the less number and smaller size of nanoparticles was observed in lowest metal salt concentration.

3.4 Morphological studies

3.4.1 SEM analysis

The SEM images explain the morphological study of AuNPs (a_1 , a_2 and a_3) synthesized from *J. adhatoda*. The obtained AuNPs (a_1 , a_2 and a_3) were found to be spherical shape with and without aggregation. Shape of sample a_1 is uniform, but a_2 and a_3 samples are poly-dispersed in nature with slight aggregation are shown in Fig. 5a–c.

3.4.2 TEM analysis

The size and shape of the nanoparticles were further confirmed by TEM analysis. The TEM images in Fig. 6a–f prove the synthesized AuNPs are spherical in shape and their average sizes are 27.1, 33.3 and 46.8 nm for sample a_1 , a_2 and a_3 respectively. Some AuNPs are agglomerated in some places, thereby indicating possible deposition of nanoparticles after few days. Philip et al. [16, 60, 61] also discussed that the synthesized spherical shape of gold nanoparticles is due to the sharp SPR peak. TEM images also confirmed that the spherical shape and its sizes was increased with increase in the concentration of HAuCl_4 . Beside, analysis of the AuNPs by Energy Dispersive

Spectroscopy (EDAX) confirmed the occurrence of the signal feature of elemental gold (Fig. 6g). Maximum peaks are noticed for crystalline Au peaks and few peaks are observed for Cu comes from the copper grid. Thus, there are no foreign substances present in the sample. Figure 6h shows Selected Area Electron Diffraction pattern (SAED) of the AuNPs and it is measured from one of the nanoparticles. The SAED images clearly exhibited the diffraction rings with interplanar spacing which denotes AuNPs are crystalline nature. SAED spots are related to the different crystallographic planes of FCC structure of elemental gold (Fig. 6h) The SAED spots are related to the different crystallographic plane families [111], [200] and [220] of pure face-centred cubic gold structure [62].

3.5 Xrd

The typical XRD pattern of fabricated AuNPs displayed, Bragg's reflection planes at (111), (200), (220) and (311) corresponds to 2θ values of the peaks at 38.3° , 44.3° , 64.5° and 77.6° respectively (Fig. 7) for a_1 – a_3 . All peaks of AuNPs (a_1 – a_3), which are well matched with the standard data file (JCPDS file No. 99-101-3542). From this result, a number of prominent Bragg reflection peaks are based on Face Centered Cubic (FCC) crystalline nature of AuNPs. The reflection peaks are broader which indicates the smaller dimension of particles [63]. No other peaks are found in XRD pattern, which is confirmed the purity of AuNPs. Hence, the obtained pure crystalline nature of AuNPs was enclosed with biomolecules.

The peak (38.3°) corresponding plane is more intense than other planes. Thus, the plane is signifying one; this is due to the predominant progress of AuNPs along the direction of plane (111). The average nanocrystallite size is calculated by using Debye–Scherrer equation and it is found to be 20.2, 40.1 and 40.3 nm for the corresponding samples a_1 , a_2 and a_3 respectively, which slightly varied from the obtained particle sizes of TEM analysis of AuNPs (Fig. 6a–f). It shows slight changes of the spherical shape of particles that is needed the Debye–Scherrer formula.

The average nanocrystalline material size has been calculated by Debye–Scherrer formula,

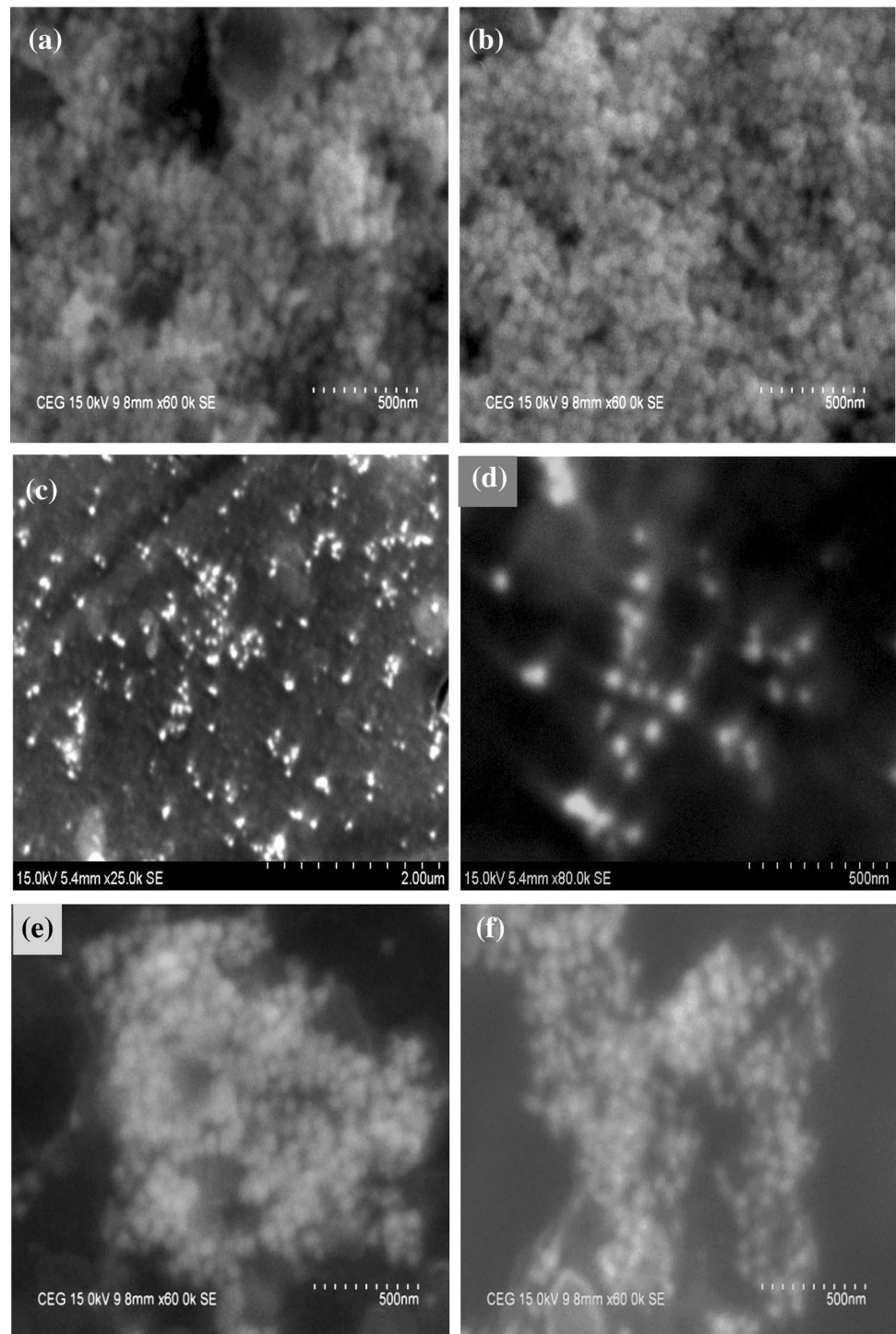
$$D = k\lambda / \beta \cos \theta,$$

where D is particle diameter size, $k = 1$ (constant), λ wavelength of X-ray source (0.1541 nm), β full width at half maximum (FWHM) and θ diffraction angle corresponding to the lattice plane (111).

3.6 FTIR

In order to inspect the AuNPs, they are capped with the biomolecules. FTIR analysis was carried out in order to

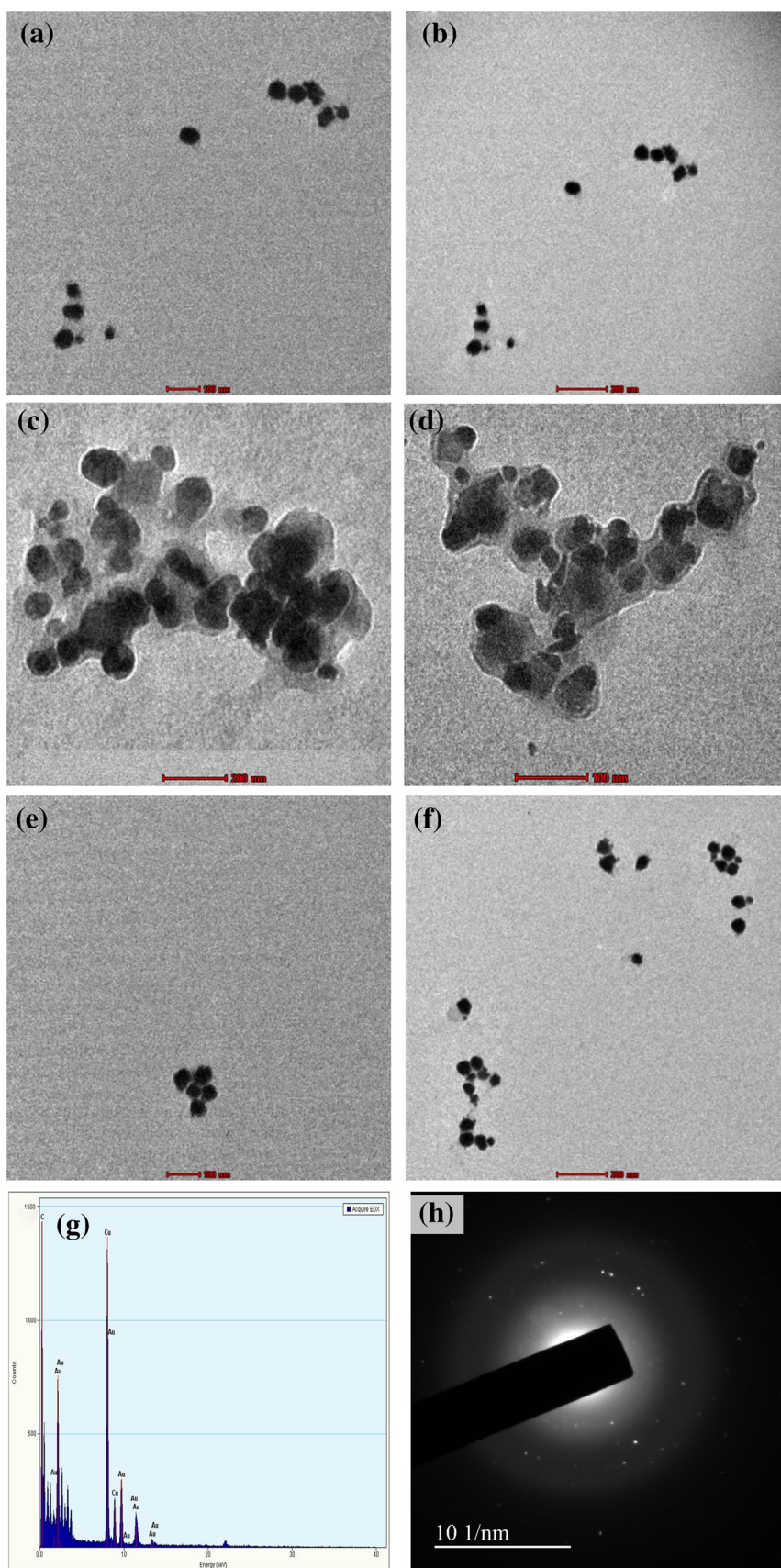
Fig. 5 SEM images of AuNPs from *J. adhatoda* leaf extract **a** a₁, **b** a₂ and **c** a₃



detect the potential biomolecules of *J. adhatoda* plant extract which are responsible for the reduction, capping and efficient stabilization of AuNPs. FTIR spectrum of aqueous leaf extract shows the stretching vibration peaks at 3404, 2938, 2846, 1636, 1408, 1050, 1257, 1082, 827 and 886 cm^{-1} (Fig. 8a). The synthesized AuNPs exhibit the peaks at 3402, 2850, 1636, 1404, 1081, 661, 600 and

522 cm^{-1} (Fig. 8b). The broad IR band at 3402 cm^{-1} is due to stretching vibrations of O–H group [64]. A peak at 1634 cm^{-1} is attributed to C–O stretching vibrations in the amide I shifted to 1636 cm^{-1} the protein molecules are possible to bind with AuNPs via carboxylate groups ($-\text{COO}^-$) [25, 64–66]. The peak at 1408 cm^{-1} is due to COO^- symmetric stretching of chloroplasts shifted to

Fig. 6 TEM images of AuNPs synthesized from *J. adhatoda* leaf extract **a, b** a₁, **c, d** a₂, **e, f** a₃, **g** EDX and **h** SAED



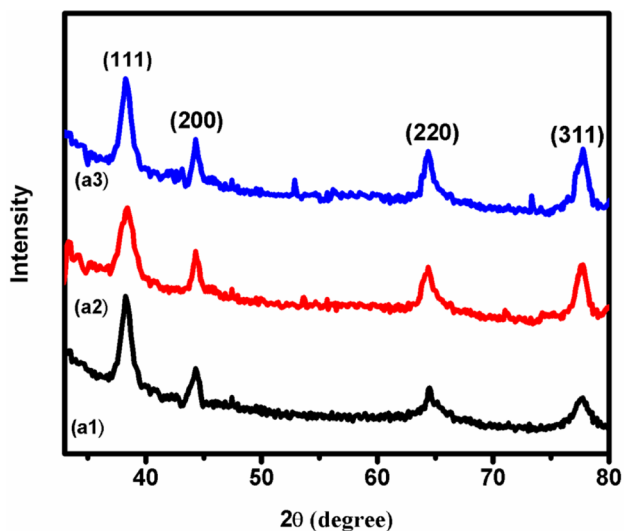


Fig. 7 XRD pattern of AuNPs for a a₁, b a₂ and c a₃

O–H (3402 cm^{-1}) and (NH) C=O groups (1636 cm^{-1}) can bind with AuNPs [25, 64]. Based on the above mentioned facts, it is confirmed that the reducing sugar (*D*-glucoside) and protein molecules are responsible for reduction of Au^{3+} and capping agent of AuNPs.

3.7 Catalytic activity studies

3.7.1 Catalytic activity of synthesized gold nanoparticles in Congo red

The present study demonstrates the size-dependent, catalytic activity of AuNPs against Congo red dye in the presence of the NaBH_4 . The absorption band of Congo red is about 486–498 nm [39]. The absorption peak of Congo red was observed at 496 nm and the peak intensity decreased during the reduction. This is due to the degradation of Congo red by AuNPs in the presence of NaBH_4 . Schematic diagram exhibits the possible structure of Congo

Fig. 8 FTIR spectra of a *J. adhatoda* plant and b AuNPs

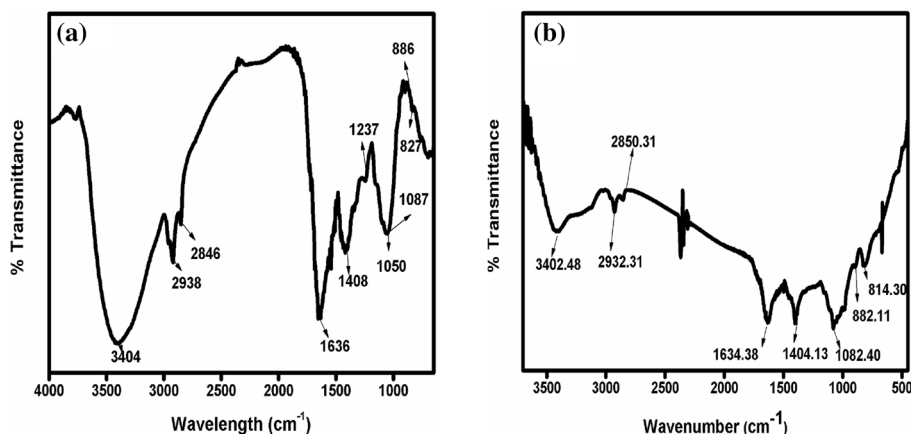
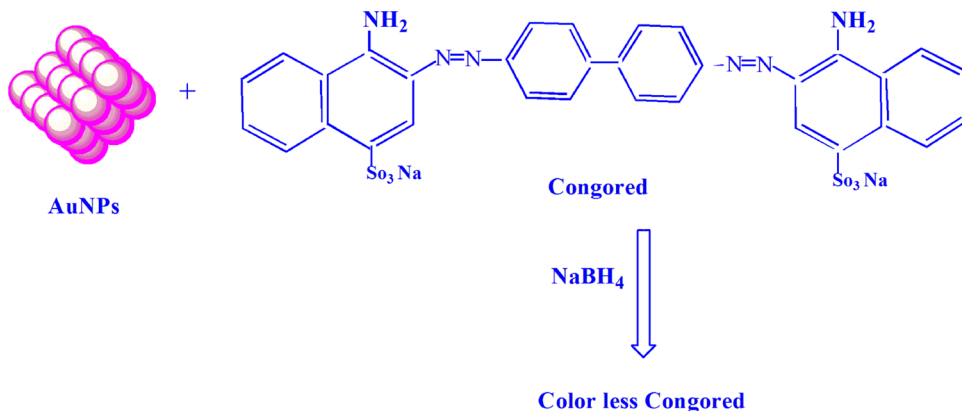


Fig. 9 Schematic diagram for Congo red degraded into protonated Congo red in the presence of synthesized AuNPs



1404 cm^{-1} [67]. A minor peak at about 661 cm^{-1} is due to C–Cl or C–Br stretch of alkyl halides [68]. In FTIR, such kind of shifting vibrational spectra has been ascribed that the

red dye degradation (Fig. 9). Figure 10a, b illustrates the catalytic degradation of Congo red by using two different

Fig. 10 UV–Vis spectra for degradation of Congo red dye without using AuNPs in the presence of **a** 0.1 M and **b** 0.2 M NaBH_4

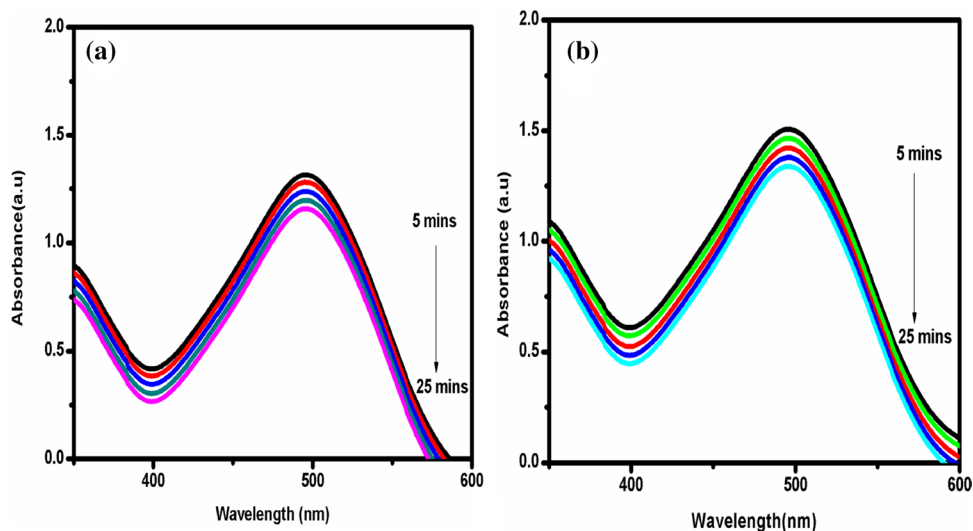
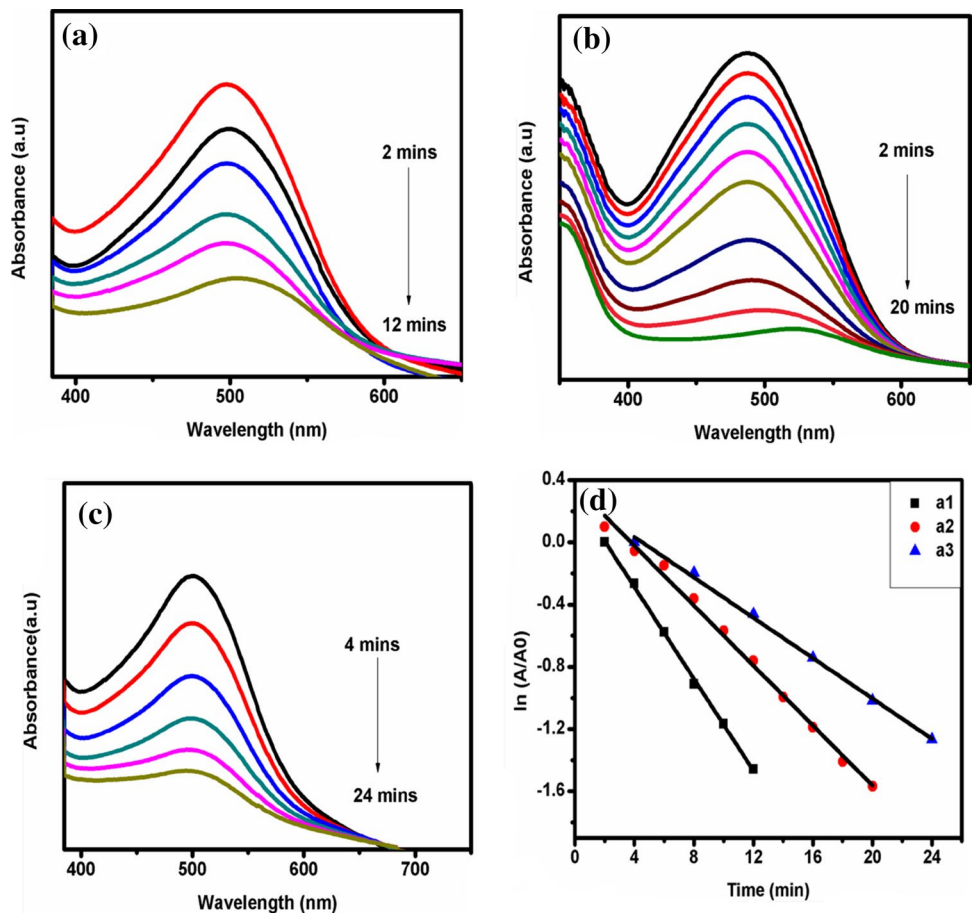


Fig. 11 UV–Vis spectral analysis of Congo red using NaBH_4 (0.1 M) with addition of 500 μL of AuNPs **a** a_1 , **b** a_2 , **c** a_3 and **d** linear plot of kinetic data for a_1 – a_3 samples



concentrations of NaBH_4 (0.1 and 0.2 M) in the absence of AuNPs independently. The degradation was slow in both cases when increasing the concentration of NaBH_4 (0.1 and 0.2 M) meanwhile after addition of AuNPs, the degradation

was faster. Narayanan et al. [69–71] discussed that NaBH_4 is a weak reducing agent which was used in a lot of industrial processes as well as in wastewater treatment. The reduction process found to speed up by adding samples a_1 – a_3 .

Figure 11a–c shows the samples a_1 , a_2 and a_3 degraded the dye within 12, 20 and 24 min respectively. The catalytic reduction of a_1 was faster than other samples a_2 and a_3 . From this observation, the degradation time decreased while using smaller size of the nanoparticles (a_1). The sample a_1 increases the catalytic property, their larger surface area will enhance the catalytic activity [72, 73]. A good linear correlation was observed between $\ln(A/A_0)$ versus time (Fig. 11d). The overall reduction reaction was hypothetical pseudo first order reaction. The rate of reaction also increased with decrease in nanoparticles sizes [5]. The obtained rate constant values from the plot $\ln A/A_0$ versus time for all five samples are shown in Table 1. The electron transfer from donor (BH_4^-) to acceptor (Congo red dye) through the surface of AuNPs [39]. The plant extract having different functional groups are enhancing the catalytic

activity of AuNPs [74]. This study exhibits an overwhelming performance as a catalyst, depending on its size.

3.7.2 Catalytic activity of synthesized AuNPs in Methylene blue

The catalytic activity of AuNPs was demonstrated by the degradation of Methylene blue along with $NaBH_4$. The absorbance peak of Methylene blue was observed at 664 nm and with a shoulder peak at 614 nm is due to $n-\pi^*$ transition. The decreasing tendency of maximum absorption denotes the reduction of Methylene blue [72]. A possible mechanism for Methylene blue dye degradation has shown in schematic diagram in Fig. 12. Figure 13a and b demonstrate the UV–Vis absorption spectra of the reduction of Methylene blue by using two various concentrations of reducing agent (0.1 and 0.2 M) without adding AuNPs. The degradation was slow in 30 min period of time even increasing the concentrations of $NaBH_4$ [39, 40]. When adding AuNPs (a_1 – a_3) to the reaction mixture the reduction was fast respectively. Hence, the reduction reaction was found to be faster in sample a_1 rather than a_2 and a_3 samples. The degradation of dye when using a_1 , a_2 and a_3 samples within 5, 8 and 15 min respectively (Fig. 14a–c). Based on the above observation, that the degradation time was decreasing with decrease in the

Table 1 Rate constants of Congo red dye reduction

Sample code	Conc of $NaBH_4$ (M)	Volume of AuNPs (μ L)	Rate constants (min^{-1})	R^2 value
a_1	0.1	500	0.1475	0.99854
a_2	0.1	500	0.09633	0.99407
a_3	0.1	500	0.06486	0.99707

Fig. 12 Schematic diagram for Methylene blue degraded into Leuko Methylene blue in the presence of synthesized AuNPs

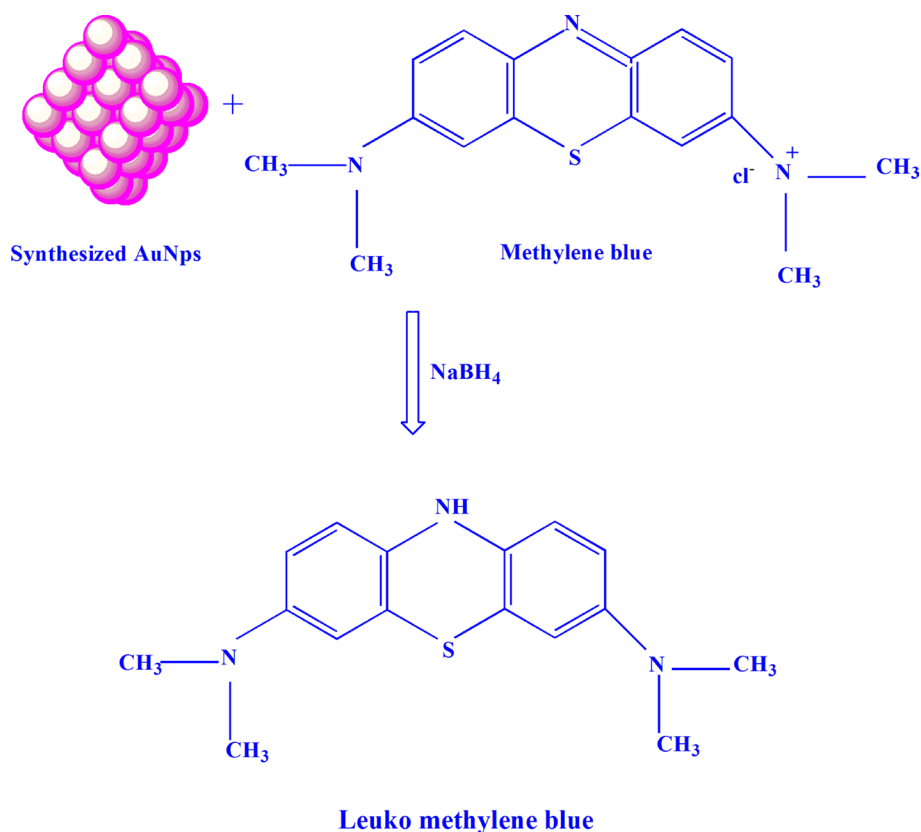


Fig. 13 UV–Vis analysis for the degradation of Methylene blue without addition of AuNPs using different concentration of NaBH_4 **a** 0.1 M and **b** 0.2 M

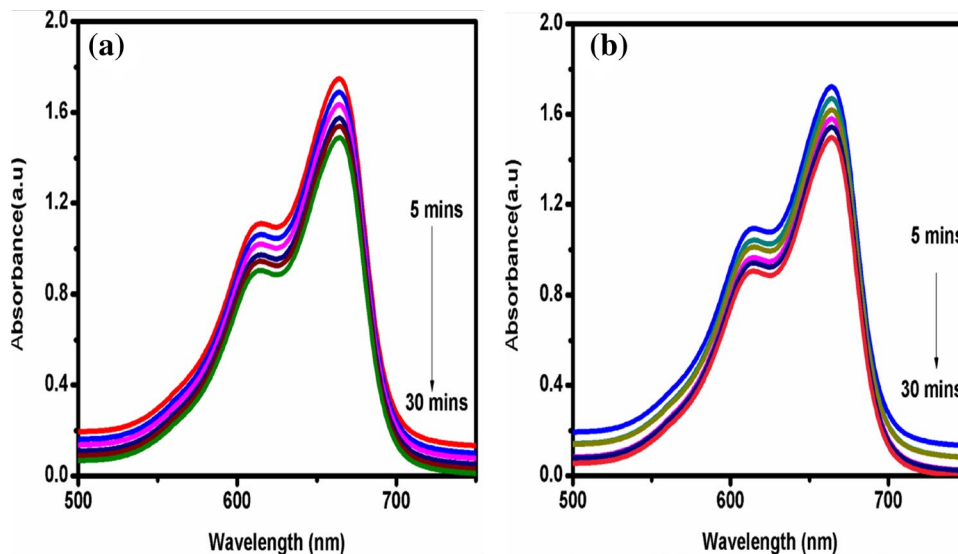


Fig. 14 UV–Vis spectra for Methylene blue using NaBH_4 with addition of 500 μL of AuNPs **a** a_1 , **b** a_2 , **c** a_3 sample and **d** linear plot of kinetic data for a_1 – a_3 samples

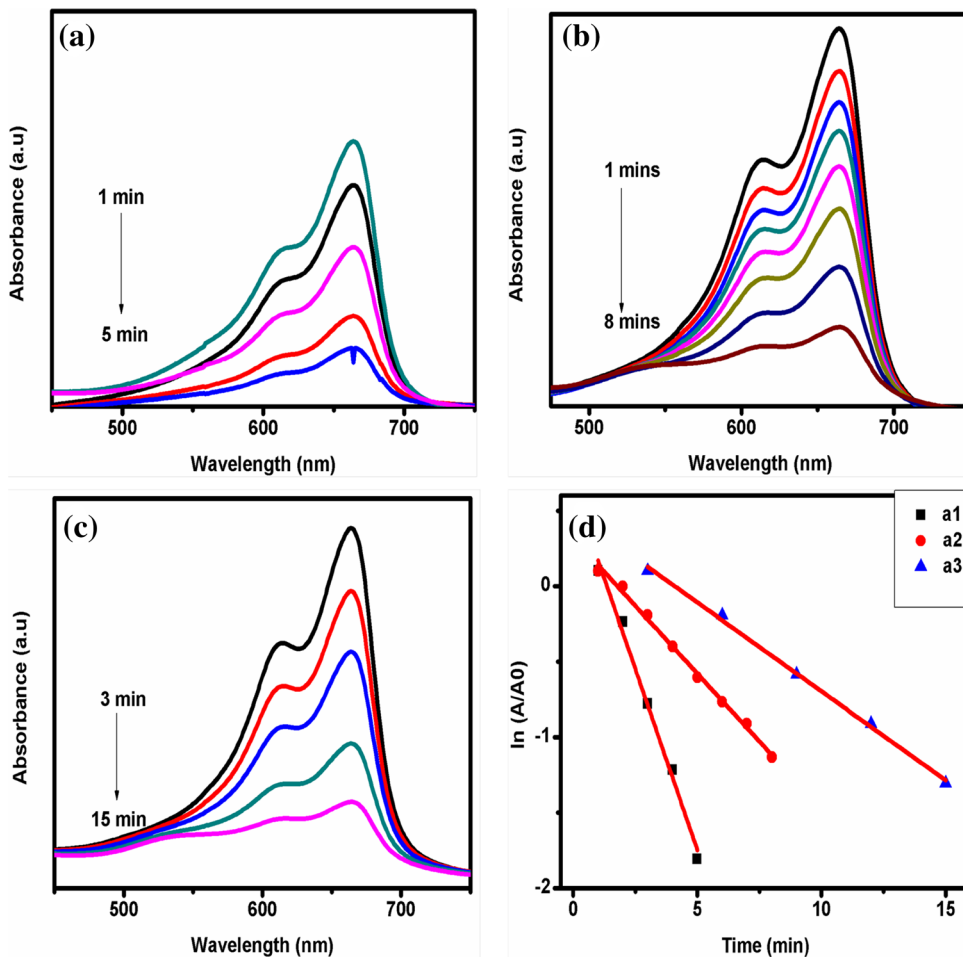


Table 2 Rate constants of Methylene blue dye reduction

Sample code	Conc of NaBH ₄ (M)	Volume of AuNPs (μL)	Rate constants (min ⁻¹)	R ² value
a ₁	0.1	500	0.47948	0.99055
a ₂	0.1	500	0.17961	0.99546
a ₃	0.1	500	0.11769	0.99716

size of AuNPs (a₁ – 27.1 nm) [39, 40]. The smaller size of AuNPs will increase the catalytic activity, due to their larger surface area [69]. The rate of reaction was also increased with decrease in nanoparticles sizes [5]. The rate of catalytic degradation increased with increase in the dosage of catalyst [75]. A good linear correlation plot was observed between ln A/A₀ versus time graph (Fig. 14d). From the plot of ln A/A₀ versus time, the rate constant values for all the five samples are shown in Table 2. AuNPs are assisting the electron transmission from donor (BH₄⁻) to acceptor (Methylene blue) in the redox reaction which is termed as an electron relay effect [71]. The percentage of dye degradation can be calculated using the following equation.

$$\% \text{ of dye degradation} = \frac{A_0 - A}{A_0} \times 100$$

A₀ initial absorbance, A absorbance at time.

Therefore, the catalytic reduction reactions (Congo red and Methylene blue), was carried out as-synthesized AuNPs acted as a potential catalyst. Table 3 represents a comparative literature survey of dye degradation, against Congo red and Methylene blue by different nanoparticles.

4 Conclusion

We disclosed an ecofriendly approach for synthesis of stable AuNPs using *J. adhatoda* leaf extract. The concentration of metal was essential in synthesis of various sizes

of AuNPs. The spherically crystalline nature of AuNPs was encircled with the D-gulcoside and protein molecules. When there is increase in concentration of reducing agent, the degradation did not show better results, meanwhile after the addition of AuNPs, the degradation was good. Then, the obtained AuNPs was efficient in catalytic dye degradation. This study reveals that the smaller size of AuNPs enhances the catalytic activity due to their large surface area. From the above result, we concluded the most excellent degradation was found in Methylene blue than Congo red. Finally, green synthesized AuNPs are effective nano-catalyst and could be made potentially exciting for large scale synthesis of AuNPs.

Acknowledgements We acknowledge the support extended by University of Madras, IIT, Chennai and TNAU, Coimbatore, India for providing research facilities.

Compliance with ethical standards

Conflict of interest The authors declare that they have no competing interests.

References

- Philip D (2010) Honey mediated green synthesis of silver nanoparticles. *Spectrochim Acta A* 77:807–810
- Rai M, Gade AY (2011) Biogenic nanoparticles: an introduction to what they are how they are synthesized and their applications. Springer, Berlin, pp 12–26
- Raveendran P, Fu J, Wallen S-L (2003) Completely “Green” synthesis of metal nanoparticles. *J Am Chem Soc* 125:13940–13941
- Park Y, Hong Y-N, Weyers A, Kim Y-S, Linhardt R-J (2011) Polysaccharides and phytochemicals: a natural reservoir for the green synthesis of gold and silver nanoparticles. *IET Nanobiotechnol* 5(3):69–78
- Suwith V-S, Philip D (2014) Catalytic degradation of Methylene blue using biosynthesized gold and silver nanoparticles. *Spectrochim Acta A* 118:526–532
- Daniel M-C, Astruc D (2004) Gold nanoparticles: assembly supra molecular chemistry quantum-size related properties and

Table 3 Review of various nanoparticles utilized for degradation of Methylene blue (MB) and Congo red dye (CR)

S. No	Source	Nano particles	Dye	Time (min)	Rate constant (min ⁻¹)	Author
1	<i>Saraca indica</i>	AgNps	MB	12	0.4416	[73]
2	<i>Brassica rapa</i>	AuNPs	MB	18	0.372	[69]
3	<i>Salmaliamaala barica gum</i>	AuNPs	MB	9	0.241	[58]
			CR	10	0.236	
4	<i>Amaranthus gangeticus</i>	AgNps	CR	15	–	[76]
5	<i>Mushroom</i>	AuNPs	MB	23	0.0529	[77]
6	<i>Bacillusmaris flavi</i>	AuNPs	CR	20	0.2192	[39]
7	<i>Justicia adhatoda</i>	AuNPs	CR	12	0.1475	Present study
			MB	5	0.47948	

- applications towards biology catalysis and nanotechnology. *Chem Res* 104:293–346
7. John Paul J, Aseniero Einstine, Piso MO, Banda MHT, Tabelin CB (2019) Potential utilization of artisanal gold-mine tailings as geopolymeric source material: preliminary investigation. *SN Appl Sci* 1:35
 8. Alaqad K, Saleh T-A (2016) Gold and silver nanoparticles: synthesis methods, characterization routes and applications towards drugs. *J Environ Anal Toxicol* 6(4):1000384
 9. Jafarizad K, Safae S, Gharibian Y, Omid D, Ekinci D (2015) Biosynthesis and in vitro study of gold nanoparticles using mentha and pelargonium extracts. *Proc Mat Sci* 11:224–230
 10. Grumezescu A-M, Sengani M, Rajeshwari V-D (2017) Recent trends and methodologies in gold nanoparticle synthesis—A prospective review on drug delivery aspect. *Open Nano* 2:37–46
 11. Iqbal M, Usanasea G, Oulmib K, Aberkaneb F, Bendaikhab T, Fessia H, Zinec N, Agustia G, El-S Errachidc, Elaissari A (2016) Preparation of gold nanoparticles and determination of their particles size via different methods. *Mat Res Bul* 79:97–104
 12. Han L-S, Kyu J-H, Cheol K-T, Hee K-C, Hwan S-C, Tae-Sik Y, Ra H-A, Seong J-H, Hun K-D (2018) Facile method for the synthesis of gold nanoparticles using an ion coater. *Appl Sur Sci* 434:1001–1006
 13. Song J-Y, Jang H-K, Kim B-S (2009) Biological synthesis of gold nanoparticles using *Magnolia kobus* and *Diopyros kaki* leaf extracts. *Proc Biochem* 44:1133–1138
 14. Majumdar R, Bag B-J, Maity N (2013) *Acacianilotica* (Babool) leaf extract mediated size controlled rapid synthesis of gold nanoparticles and study of its catalytic activity. *Int Nano Lett* 3:53
 15. Sett A, Gadewar M, Sharma P, Deka M, Bora U (2016) Green synthesis of gold nanoparticles using aqueous extract of *Dilleniaindica*. *Adv Nat Sci Nanosci Nanotech* 7:025005
 16. Philip D (2009) Honey mediated green synthesis of gold nanoparticles. *Spectrochimica Acta A* 73:650–653
 17. Smitha S-L, Philip D, Gopchandran K-G (2009) Green synthesis of gold nanoparticles using *Cinnamomumzey lanicum* leaf broth. *Spectrochimica Acta Part A* 74:7
 18. Pathak R-P (1970) Shri Ramdayal Joshi Memorial Ayurvedic Research Institute 1:121
 19. Singh T-P, Singh O-M, Singh H-B (2011) *Adhatodavasica* Nees: phytochemical and pharmacological profile. *Nat Prod J* 1:29–39
 20. Dhankhar S, Kaur R, Ruhil S, Balhara M, Dhankhar S, Chhillar A-K (2011) A review on *Justiciaadhatoda*: a potential source of natural medicine. *Afri J Plant Sci* 5(11):620–627
 21. McMullan G, Meehan C, Conneely A, Kirby N, Robinson T, Nigam P, Banat I-M, Marchant R, Smyth WF (2001) Microbial decolorization and degradation of textile dyes. *Appl Microbiol Biotechnol* 56:81–87
 22. Pearce C-I, Lloyd J-R, Guthrie J-T (2003) The removal of colour from textile wastewater using whole bacterial cells: a review. *Dyes Pigments* 58:179–196
 23. Lee J-W, Choi S-P, Thiruvengkatachari R, Shim W-G, Moon H (2006) Evaluation of the performance of adsorption and coagulation processes for the maximum removal of reactive dyes. *Dyes Pigments* 69(3):196–203
 24. Rafi F, Franklin W, Cerniglia CE (1990) Azoreductase activity of an aerobic bacteria isolated from human interstitial microflora. *Appl Environ Microbiol* 56:2146–2151
 25. Sodeinde O, Eboeime U (2013) Adsorption of textile wastes containing Methylene blue and congo red using activated carbon produced from coconut shell. *Int J Computat Eng Manag* 16(5):2230–7893
 26. Yang G, Wu L, Xian Q, Shen F, Wu J, Zhang Y-Z (2016) Removal of congo red and Methylene blue from aqueous solutions by vermicompost-derived. *Biochars PLoS ONE* 11(5):0154562
 27. Gillman P-K (2006) Methylene blue implicated in potentially fatal serotonin toxicity. *Anaesthesia* 61:1013–1014
 28. Oliveira L-S, Franca A-S, Rocha S-D, Alves M-T (2008) Evaluation of untreated coffee husk as potential biosorbent for treatment of dye contaminated water. *J Harz Mat* 155(3):507–512
 29. Raymundo A-S, Zanarotto R, Belisário M, Pereira M-G, Ribeiro J-N, Ribeiro A (2010) Evaluation of sugar-cane bagasse as bioadsorbent in the textile waste water treatment contaminated with carcinogenic congo red dye. *Braz Arch Biotechnol* 53(4):931–938
 30. Banat I-M, Nigam P, Singh D, Marchant R (1996) Microbial decolorization of textile dye containing effluents. *Bioresour Technol* 58:217–227
 31. Han R Zhang J, Zou W, Shi J, Liu H (2005) Equilibrium biosorption isotherm for lead ion on chaff. *J Harz Mat* 125(1–3):266–271
 32. Ho Y-S, Chiu W-T, Wang C-C (2005) Regression analysis for the sorption isotherm of basic dyes on sugar-cane dust. *Bioresour Technol* 96(11):1285–1291
 33. Kumar K-V (2006) Linear and non-linear regression for the sorption kinetics of Methylene blue onto activated carbon. *J Harz Mater* 137(3):1538–1544
 34. Ho Y-S (2006) Second-order kinetic model for the sorption of cadmium onto tree fern: a comparison linear and non-linear methods. *Water Res* 40(1):119–125
 35. Gupta V-K, Ali I, Suhas X, Mohan D-J (2003) Equilibrium uptake and sorption dynamics for the removal of a basic dye (basic red) using low-cost adsorbents. *Coll Interf Sci* 265:257
 36. Santhi T, Manonmani S, Smitha T (2010) Removal of methyl red from aqueous solution by activated carbon prepared from the *annonasquamosa* seed by adsorption. *Chem Eng Res Bull* 14:11–18
 37. Malana M-A, Ijaz S, Ashiq N (2010) Removal of various dyes from media onto polymeric gels by adsorption process: their kinetics and thermodynamics. *Desalination* 263:249–257
 38. Wang L-G, Yan G-B (2011) Adsorptive removal of direct yellow 161 dye from aqueous solution using bamboo charcoal activated with different chemicals. *Desalination* 274:81–90
 39. Nadaf N-Y, Kanase S-S (2016) Biosynthesis of gold nanoparticles by *Bacillus marisflavi* and its potential in catalytic dye degradation. *Arab J Chem* 09:20
 40. Chairam N-Y, Konkamdee W-S, Parakhun R (2017) Starch-supported gold nanoparticles and their use in 4-nitrophenol reduction. *J Saudi Chem Soc* 21:656–663
 41. Liu X, Yu L, Xie F, Li M, Chen L, Li X (2010) Kinetics and mechanism of thermal decomposition of corn starches with different amylose/amylopectin ratios. *Starch/Stärke* 62:139–146
 42. Benet W-E, Lewis G-S, Yang L-Z, Hughes D (2011) The mechanism of the reaction of the Tollens reagent. *J Chem Res* 35:675–677
 43. Liu J, Qin G, Raveendran P, Ikushima Y (2006) Facile “green” synthesis, characterization and catalytic function of D-glucose-stabilized Au nanocrystals. *Chem Eur J* 12:2131–2138
 44. Hussain S-T, Iqbal M, Mazhar M (2009) Size control synthesis of starch capped-gold nanoparticles. *J Nanopart Res* 11:1383–1391
 45. Xia Y, Sun Y (2003) Gold and silver nanoparticles: a class of chromophores with colors tunable in the range from 400 to 750 nm. *Analyst* 128:686–691
 46. Slocik J-M, Zabinski J-S, Phillips D-M, Naik R-R (2008) Colorimetric response of peptide functionalized gold nanoparticles to metal ions. *Small* 4:548–551
 47. Shankar S-S, Rai A, Ankamwar B, Singh A, Ahmad A, Sastry M (2004) Biological synthesis of triangular gold nanoparticles. *Nat Mat* 3:482–488
 48. Annadhasan M, Muthukumarasamyvel T, Muthukumarasamyvel T, Babu V-R-S, Rajenindiran N (2014) Green synthesized silver and gold nanoparticles for colorimetric detection of Hg²⁺ Pb²⁺ and Mn²⁺ aqueous medium. *ACS Sustain Chem Eng* 2:887–896

49. Vigderman L, Zubarev E-R (2012) High-yield synthesis of gold nanorod with longitudinal SPR peak greater than 1200 nm using hydroquinone as a reducing agent. *Chem Mat* 25:1450–1457
50. Iglesias S, Pastoriza-Santos I, Perez-Juste J, Rodriguez-Gonzalez B, Garciade Abajo F-J, Liz-Marzan L-M (2006) Synthesis and optical properties of gold nanodecahedra with size control. *Adv Mater* 18:2529–2534
51. Sau T-K, Murphy C-J (2004) Seeded high yield synthesis of short Au nanorods in aqueous solution. *J Am Chem Soc* 126:8648–8649
52. Zou L, Qi W, Su R, Huang R, He Z, Wang M (2013) Green synthesis of gold nanoparticles-nanocluster composite and nanostructures as linking and reducing agent. *ACS Sustain Chem Eng* 1:1398–1404
53. Noruzi M, Zare D, Khoshnevisan K, Davoodi D (2011) Rapid green synthesis of gold nanoparticles using *Rosa hybrida* petal extract at room temperature. *Spectrochim Acta A* 79:1461–1465
54. Hu M, Chen J, Li Z-Y, Au L, Hartland G-V, Li X, Marquez M, Xia Y (2006) Gold nanostructures: engineering their plasmonic properties for biomedical applications. *Chem Soc Rev* 35:1084–1094
55. Tagad CK, Dugasani S-R, Aiyer R, Park S, Kulkarni A, Sabharwal S (2013) Green synthesis of silver nanoparticles and their application for the development of optical fiber based hydrogen peroxide sensor. *Sensors Actuators B* 183:144–149
56. Shivshankar S, Ahmad A, Pasricha R, Sastry M (2003) Bioreduction of chloroaurate ions by geranium leaves and its endophytic fungus yields gold nanoparticles of different shapes. *J Mat Chem* 3:1822–1826
57. Dubey S-P, Lahtinen M, Sillanpää M (2010) Green synthesis and characterizations of silver and gold nanoparticles using leaf extract of *Rosa rugosa*. *Colloids Surf A Physicochem Eng Asp* 364:34–41
58. Ganapuram B-R, Alle M, Dadigala R, Dasari A, Maragoni V, Guttena V (2015) Catalytic reduction of Methylene blue and Congo red dyes using green synthesized gold nanoparticles capped by *salmaliamaala baricagum*. *Int Nano Lett* 5:215–222
59. Dwivedi A-D, Gopal K (2010) Biosynthesis of silver and gold nanoparticles using *Chenopodium album* leaf extract. *Colloids Surf A: Physicochem Eng Asp* 369:27–33
60. Ibrahim HMM (2015) Green synthesis and characterization of silver nanoparticles using banana peel extract and their antimicrobial activity against representative microorganisms. *J Radiat Res Appl Sci* 8:265–275
61. Verma A, Mehata M-S (2016) Controllable synthesis of silver nanoparticles using neem leaves and their antimicrobial activity. *J Radiat Res Appl Sci* 9:109–115
62. Bhattacharyya R, Roy S, Prakash O, Singh A-P, Bhattacharya T-K, Maiti P, Bhattacharyya S, Das S (2019) 0.5Zn0.5Fe₂O₄ polyurethane thin nanocomposite coating as broadband microwave absorber. *SN Appl Sci* 1:38
63. Lokina S, Stephen A, Kaviyaran V, Arulvasu C, Narayanan V (2014) Cytotoxicity and antimicrobial activities of green synthesized silver nanoparticles. *Eur J MedChem* 76:256–263
64. Adavallan K, Krishnakumar N (2014) Mulberry leaf extract mediated synthesis of gold nanoparticles and its anti-bacterial activity against human pathogens. *Adv Nat Sci Nanosci Nanotechnol* 5:025018
65. Gurunathan S, Han J, Park J-H, Kim J-H (2014) A green chemistry approach for synthesizing biocompatible gold nanoparticles. *Nanoscale Res Lett* 9:248
66. Gole C, Dash V, Ramakrishnan S-R, Sainkar A-B, Mandale M, Sastry R-M (2001) Pepsin-gold colloid conjugates: preparation characterization and enzymatic activity. *Langmuir* 17:1674–1679
67. Zhang Y-X, Zheng J, Gao G, Kong Y-F, Zhi X, Wang K, Zhang X-Q, Cui D-X (2011) Biosynthesis of gold nanoparticles using chloroplasts. *Int J Nanomed* 6:2899–2906
68. Nagaonkar D, Rai M (2015) Sequentially reduced biogenic silver-gold nanoparticles with enhanced antimicrobial potential over silver and gold monometallic nanoparticles. *Adv Mat Lett* 6(4):334–341
69. Narayanan K-B, Park H-H (2015) Homogeneous catalytic activity of gold nanoparticles synthesized using turnip (*Brassica rapa* L.) leaf extract in the reductive degradation of cationic azodye. *Korean J Chem Eng* 32(7):1273–1277
70. Rajan A, Meenakumari M, Philip D (2014) Shape tailored green synthesis and catalytic properties of gold nanocrystals. *Spectrochimica Acta Part A* 118:793–799
71. Panigrahi S, Basu S, Praharaj S, Pande J, Jana S, Pal A, Ghosh S-K, Pal T (2007) Synthesis and size-selective catalysis by supported gold nanoparticles: study on heterogeneous and homogeneous catalytic process. *J Phys Chem C* 111:4596–4605
72. AswathyAromal S, Philip D (2012) Green synthesis of gold nanoparticles using *Trigonellafoenum-graecum* and its size-dependent catalytic activity. *Spectrochim Acta A* 97:1–5
73. Vidhu V-K, Philip D (2014) Spectroscopic microscopic and catalytic properties of silver nanoparticles synthesized using *Saraca indica* flower. *Spectrochim Acta A* 117:102–108
74. Bhakya S, Muthukrishnan S, Sukumaran M, Muthukumar M, Senthilkumar T, Rao M-V (2015) Catalytic degradation of organic dyes using synthesized silver nanoparticles: a green approach. *J Bioremed Biodegrad* 6:5
75. Mukwevho N, Elvis F, Waanders F, Kumar N, Ray S-S, Mbianda X-Y (2019) Photocatalytic activity of Gd₂O₂CO₃ ZnO-CuO nanocomposite used for the degradation of phenanthrene. *SN Appl Sci* 1:10
76. Kolya H, Parthapratim M, Akhil P, Tripathy T (2015) Green synthesis of Silver nanoparticles with antimicrobial and azo dyes (Congo red) degradation properties using *Amaranthus gangeticus* Linn leaf extract. *J Anal Sci Tech* 6:3
77. Narayanan K-B, Park H-H, Han S-S (2015) Synthesis and characterization of biomatrixed-gold nanoparticles by the mushroom *Flammulin velutipes* and its heterogeneous catalytic potential. *Chemosphere* 141:169–175